PERGAMON

International Journal of Heat and Mass Transfer 45 (2002) 2423–2430

International Journal of HEAT and MASS TRANSFER

www.elsevier.com/locate/ijhmt

Experimental study of the forces associated with mixed convection from a heated sphere at small Reynolds and Grashof numbers. Part II: Assisting and opposing flows

E. Mograbi [a], G. Ziskind [a,*], D. Katoshevski [b], E. Bar-Ziv [a,c]

[a] *Department of Mechanical Engineering, Ben-Gurion University of the Negev, P.O. Box 653, Beer-Sheva, Israel*
[b] *Department of Environmental Engineering, Institute for Applied Biosciences, Ben-Gurion University of the Negev, P.O. Box 653, Beer-Sheva, Israel*
[c] *Institutes for Applied Research, Ben-Gurion University of the Negev, P.O. Box 653, Beer-Sheva, Israel*

Received 29 May 2001; received in revised form 15 November 2001

Abstract

The present paper addresses the issue of mixed convection from a small heated sphere in assisting and opposing flow configurations. The sphere is suspended in an electrodynamic chamber (EDC), where it is heated by a focused laser beam up to several hundred degrees above room temperature. As a result, free convection is induced from the sphere, with the Grashof number smaller than 0.02. A vertical forced flow is then applied and gradually increased in a quasi-static manner. The forced flow velocities are in the range 0–0.1 m/s, providing very low particle Reynolds numbers, usually less than 0.5. The effects of the free convection on the drag force experienced by the particle, and of the forced flow on the free convection are assessed quantitatively, measuring continuously the vertical forces experienced by the sphere. A similarity law developed in the previous study is successfully applied to determine the behavior of the drag force at various particle heating levels. © 2002 Published by Elsevier Science Ltd.

Keywords: Free and forced convection; Small sphere; Assisting and opposing flows

1. Introduction

Heat transfer from- or to- a body of spherical or near spherical shape is a problem of great practical importance. It arises in such important industrial applications as fuel spray and coal combustion, fluidized beds, drying, particulate technologies, and many others in which small particles are involved. As discussed in Part I of this study [1], the regime of heat transfer may be dominated by the free convection, by the forced convection, or represent comparable effects of both. It is quite common to describe the magnitude of free convection in terms of Grashof or Rayleigh numbers. As for the forced flow, the common parameter used for the analysis is the Reynolds number.

The flow associated with free convection is in the vertical direction, while the forced flow may have an arbitrary direction. Thus, it is common to study the mixed convection analyzing three basic cases:

1. "assisting", where the direction of the forced flow coincides with that of the free convection flow;
2. "opposing", where the direction of the forced flow is opposite to that of the free convection flow;
3. "crossing", where the direction of the forced flow is normal to that of the free convection flow.

While free convection from a sphere, including that at low Grashof numbers, was studied quite extensively in the past analytically [2–4], numerically [5,6] (see the book by Gebhart et al. [7] for a summary), and experimentally [8], the existing results for mixed convection are rather limited, especially for small bodies where the

* Corresponding author. Tel.: +972-8-647-7089; fax: +972-8-647-2813.
E-mail address: gziskind@bgumail.bgu.ac.il (G. Ziskind).

0017-9310/02/$ - see front matter © 2002 Published by Elsevier Science Ltd.
PII: S0017-9310(01)00350-7

Nomenclature

Bi	Biot number ($= hd/k_p$)
d	particle diameter (m)
F	force (N)
g	gravitational acceleration (m/s^2)
Gr	Grashof number ($= g\beta[T_p - T_{cold}]d^3/v^2$)
k	thermal conductivity (W/m K)
Q	volume flow rate (cm^3/min)
Re	Reynolds number ($= ud/v$)
T	temperature (K or °C)
u	velocity (m/s)
V	voltage (V)
z	Cartesian coordinate

Greek symbols

β	thermal expansion coefficient (K^{-1})
μ	dynamic viscosity (kg/m s)
v	kinematic viscosity (m^2/s)
ρ	density (kg/m^3)

Subscripts

cold	surroundings
f	film
d	drag
g	gas
p	particle
∞	ambient

Reynolds and Grashof numbers are small. A pioneering experimental work on the mixed-convection heat transfer from a sphere in cross-flow was performed by Yuge [9]. Hieber and Gebhart [10] studied analytically mixed convection in assisting and opposing flows. Correlations were proposed [11] for the Nusselt number in the region where $1 < Gr_p < 10^5$, $3.5 < Re_p < 5.9 \times 10^5$, corresponding to the results of Yuge [9].

The present study deals with the assisting and opposing flow cases of mixed convection, shown schematically in Fig. 1. When the forced flow is weak, the free convection dominates. When the forced flow is strong enough, it eliminates the free convection, and the flow around the hot sphere becomes similar to that around a cold one.

The cross-flow regime of mixed convection has been extensively studied in Part I of the present investigation [1]. The experimental method was based on a novel technique developed by the authors for the study of various physical phenomena related to a single small heated particle levitated in an electrodynamic chamber (EDC) [1,12,13]. It has been shown both qualitatively and quantitatively how the free and forced convection interact when one of them dominates over the other, and when there are comparative contributions of both. A power law has been established for generalization of the results concerning both the hydrodynamic drag force acting on a heated particle, and the force resulting from the free convection flow around the particle.

In the present work, both the assisting and the opposing cases of mixed convection are investigated by the same method. The regimes predominated by free and forced convection are considered along with the regimes where the contributions from free and forced convection are comparable to each other.

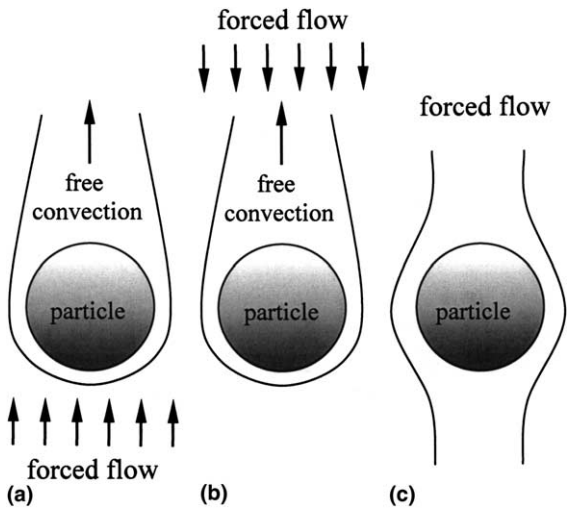

Fig. 1. Mixed convection from a heated sphere in the assisting and opposing flows.

2. Experimental method

The experimental system and measurement procedure has been described in detail in the past [1,12,13], and only a brief description appears here.

A charged particle can be levitated by an electric field inside the EDC. The design of the experimental apparatus enables to balance various external forces (weight, drag, photophoresis) by the electric field that, in turn, can be directly measured.

When only gravity, which is directed downwards, is applied, the vertical electric force balances the force of gravity, mg. When a focused laser beam irradiates the particle, free convection is generated, producing the upward directed force, F_{fc}, because the particle is hotter than its surroundings. When a forced flow is applied in the vertical direction, it exerts the drag force, F_d, on the particle. Thus, in a general case of assisting/opposing mixed convection, the electric field balances a combi-

nation of gravity and the contributions from free and forced convection. Unlike the gravity, these contributions cannot be separated, as discussed below.

It is important to note that while the experimental set-up is generally the same as used in Part I, the EDC had to be modified since it was originally designed for a horizontal forced flow only. The new design of the chamber made the flow in both directions along the vertical z-axis possible.

As in Part I, we use smooth spherical glassy-carbon particles, in the size range 80–105 μm in diameter, because of their strong chemical resistivity to oxidation at the operating temperature range (300–600 K in the present work).

A typical experiment both for the assisting and opposing regimes is carried out in the following way: a particle is charged and levitated in the EDC to a fixed position. Its weight is balanced by the electric field in the z-direction. Then, the nitrogen flow is started. The flow rate is increased very slowly, providing a quasi-static process. The increasing drag force exerted on the particle is balanced by the electric field in the z-direction. It is important to note that the EDC controller maintains the particle at a fixed position regardless of the flow rate level. Thus, a dependence of the force on the flow rate is obtained first for an unheated particle.

Then, the particle is heated, at a zero forced flow, by a focused CO_2 laser beam to a certain temperature level, depending on the applied laser power. The heating causes free convection around the particle that "reduces" the particle weight. Accordingly, the electric force in the z-direction is adjusted automatically to balance the force of free convection. Then, the nitrogen flow is started and increased slowly, while the heating level is kept constant, and the force experienced by the heated particle is obtained.

3. Results and discussion

3.1. Raw experimental data

Typical raw experimental results are shown in Figs. 2 and 3 for the assisting and opposing regimes, respectively. The results are presented for a typical 80 μm particle as measured in the experiments, i.e. voltage versus volume flow rate, for different laser power values. As in the previous study, special care was given to high resolution with respect to the flow rate, and each curve presented in the figures contains about two thousand measured points. In every case, one curve (squares) represents the results for an unheated particle. The other curves represent five different heating levels, established by applying laser power of: 2, 3, 5, 7, and 9 W. The flow rate inside the chamber varied from 0 to 100 cm^3/min.

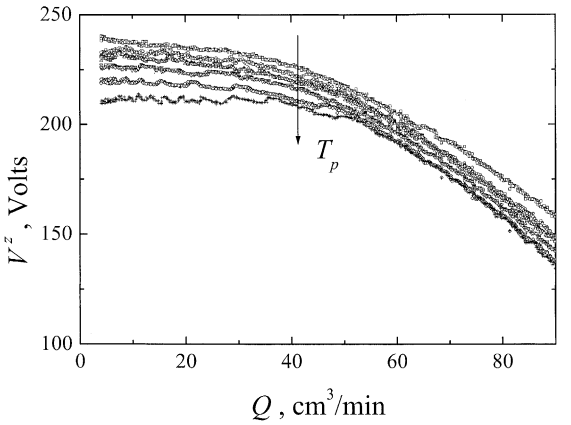

Fig. 2. Assisting flow: the voltage necessary to balance the drag force in the z-coordinate at different heating levels, as a function of flow rate: (□) no heating; (◯) heating power of 2 W; (△) heating power of 3 W; (▽) heating power of 5 W; (◇) heating power of 7 W; (+) heating power of 9 W. The arrow indicates an increase in particle temperature. The same legend applies also to Figs. 3–10.

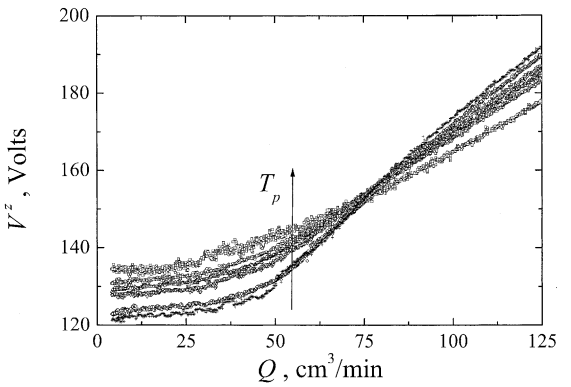

Fig. 3. Opposing flow: the voltage necessary to balance the drag force in the z-coordinate at different heating levels, as a function of flow rate. The arrow indicates an increase in particle temperature.

Fig. 2 represents the voltage, V^z, needed to keep a particle in the center of the EDC chamber when the *assisting* forced flow is imposed in the vertical direction, from the bottom to the top of the chamber. When the forced flow is zero, the voltage $V^z_{\mathrm{hot},0}$ balances the sum of gravity and free convection for the heated particle, while the voltage $V^z_{\mathrm{cold},0}$ balances the gravity alone. Since the drag exerted by the forced flow is opposite to the gravity, the voltage, V^z, decreases as the volume flow rate, Q, increases, corresponding to an increase in drag force with flow velocity. This pattern is repeated for any of the heating levels.

Fig. 3 shows the voltage, V^z, needed to levitate a particle when the *opposing* forced flow is imposed in the vertical direction, from the top to the bottom of the chamber. For a zero forced flow, the physical picture is, obviously, the same as in Fig. 2. For a nonzero forced flow, the drag acts in the same direction as the gravity. Therefore, the voltage, V^z, increases as the volume flow rate, Q, increases, corresponding to an increase in drag force with flow velocity. Here, as well, the same pattern is repeated for any of the heating levels.

Since the same particle is used, the voltages $V^z_{\mathrm{cold},0}$ should have been identical in Figs. 2 and 3, provided the charge of the particle is exactly the same. It is, however, impossible to assign the same charge to a particle in two different experiments. For this reason, a charge-elimination procedure, discussed in [12,13], is used in the analysis.

As the weight of the particle is known, one can introduce the relative vertical force, normalized with the particle weight, as follows:

$$\frac{F_z}{mg} = \frac{V^z}{V^z_{\mathrm{cold},0}}. \tag{1}$$

Moreover, since the weight is constant, it can be subtracted from the vertical force, yielding the hydrodynamic drag, i.e. the combined contribution of free and forced convection, as

$$F_{\mathrm{d}} = F_z - mg, \tag{2}$$

where the measured voltages are used to obtain the following relation:

$$\frac{F_{\mathrm{d}}}{mg} = \frac{V^z - V^z_{\mathrm{cold},0}}{V^z_{\mathrm{cold},0}}. \tag{3}$$

The ratio $V^z/V^z_{\mathrm{cold},0}$ is measured with experimental uncertainty smaller than 0.2%.

The normalized hydrodynamic force, F_{d}/mg, defined from Eq. (3), is shown in Figs. 4 and 5 for the assisting and opposing flow regimes, respectively. One can see from Fig. 4 that for the assisting flow, the hydrodynamic force is larger for a hotter particle, at any specific forced flow rate. When the free convection dominates, this behavior of the force is because the hotter particle causes a stronger free convection flow around it. Such a behavior is also found when the forced convection dominates, since the hydrodynamic force at a fixed flow rate depends linearly on the viscosity of the gas, which is larger at higher particle temperatures. As a result, the curves in Fig. 4 which correspond to different heating levels follow the same pattern.

Fig. 5 represents the hydrodynamic force acting on the same particle, as in Fig. 4, but in the opposing flow. The *absolute* values of the forces behave in the same way in the two extreme cases, namely, when the free convection dominates and when the forced convection dominates, the force for the same flow rate is smaller when the heating is lower. However, since the directions of the free and forced flows are opposite, there exists, for each heating level, a critical forced flow rate at which the net hydrodynamic force is 0. One can see from the figure that the curves corresponding to different heating levels cross one another.

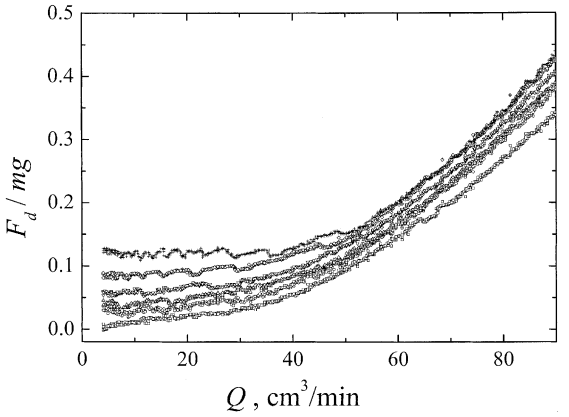

Fig. 4. Assisting flow: the drag force acting on a heated particle at different heating levels, as a function of flow rate.

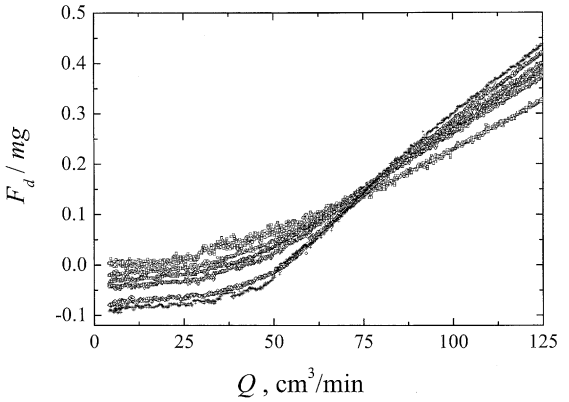

Fig. 5. Opposing flow: the drag force acting on a heated particle at different heating levels, as a function of flow rate.

The free convection force in the investigated range of particle temperatures reaches about 12% of the particle weight. Note that the maximum drag force experienced by the particle in our experiments is about 40% of the particle weight.

3.2. Dimensional analysis

Since the forces acting on a particle are determined directly from the experimental results, the first step is to find the ratio of the drag force acting on the heated particle to the drag force acting on the cold one. This

ratio can be expressed directly from the measured voltages in the vertical direction, as follows:

$$\frac{F_d}{F_{d,cold}} = \frac{V^z - V^z_{cold,0}}{V^z_{cold} - V^z_{cold,0}}, \tag{4}$$

where the index "0" stands for zero forced flow. The results of Eq. (4) are obtained experimentally within uncertainty smaller than 0.4%.

The results shown in Figs. 6 and 7 are for the assisting and opposing flow configurations, respectively. Note that the curve for the cold particle is represented by a straight line which is parallel to the horizontal axis and crosses the vertical axis at unity.

For the assisting flow, presented in Fig. 6, the curves corresponding to different heating levels behave similar to each other. Each curve descends monotonically until it becomes parallel to the line $F_d/F_{d,cold} = 1$. As shown in Part I of the present study [1], this asymptotic value is reached when free convection is fully suppressed by the forced flow. Note that as shown in Fig. 7, the asymptotic behavior of the opposing flow is similar. This is because when the free convection is suppressed, there should be no difference between the assisting, opposing, and crossing flows.

In order to generalize the experimental results, the flow rate as measured in the experiments should be first replaced by the velocity, and then by the Reynolds number. This procedure is based on the well-known Stokes relation between the velocity and the drag force acting on a sphere at low Reynolds numbers, $Re_p = ud\rho_g/\mu_g < 0.5$, under isothermal conditions

$$F_d(T_\infty) = 3\pi d\mu_g(T_\infty)u, \tag{5}$$

where μ_g and ρ_g are the dynamic viscosity and density of the gas, respectively, d is the particle diameter, u is the flow velocity when the particle is motionless, and T_∞ is the temperature of both the particle and the fluid.

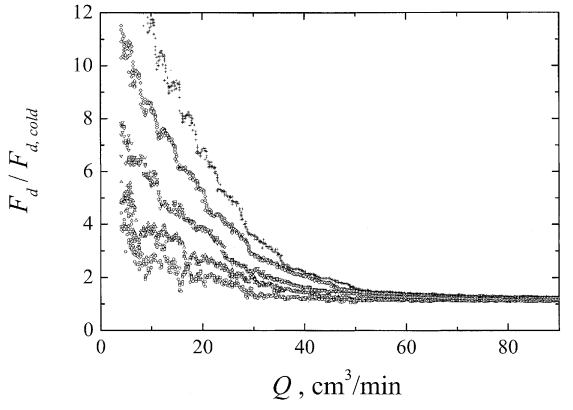

Fig. 6. Assisting flow: the hot to cold drag force ratio at different heating levels, as a function of flow rate.

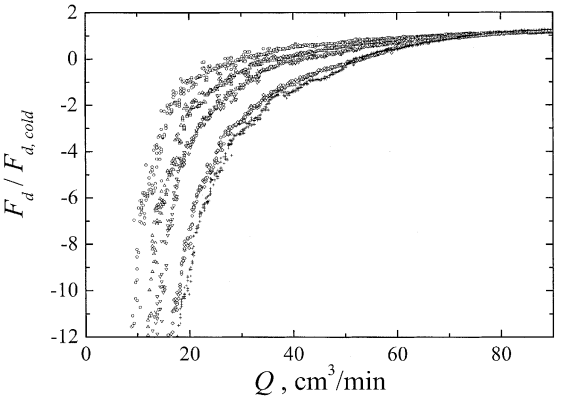

Fig. 7. Opposing flow: the hot to cold drag force ratio at different heating levels, as a function of flow rate.

Assuming that the Reynolds numbers in our case are low, as indeed shown later, Eq. (5) is used for velocity determination from the drag force. For an unheated particle, the ratio drag/weight is measured as the ratio $V^z_{cold}/V^z_{cold,0}$. Since for a smooth sphere this ratio is given by $F_d/mg = 18\mu_g u/d^2\rho_p g$, the velocity is readily calculated from

$$u = \frac{\rho_p g d^2}{18\mu_g}\frac{V^z_{cold}}{V^z_{cold,0}}, \tag{6}$$

where $\rho_p = 1450$ kg/m^3 is the density of glassy carbon particles. Knowing the value of the flow velocity, u, a corresponding value of the particle Reynolds number, Re_p, is readily calculated. Thus, it becomes possible to plot the measured forces versus the Reynolds number.

A similar procedure can be used for particle temperature estimation [1,13]. For a heated particle, when the forced flow dominates but is still in the Stokes regime, the ratio of forces tends to the ratio of the viscosities,

$$\frac{F_d}{F_{d,cold}} \to \frac{\mu_g(T_{film})}{\mu_g(T_{cold})}, \tag{7}$$

where $\mu_g(T_{film})$ is the dynamic viscosity of the gas at the film temperature given by $T_{film} = (T_p + T_{cold})/2$. This is because when the forced flow dominates, the Stokes relation can be used in a slightly modified form [13]

$$F_d = 3\pi d\mu_g(T_{film})u. \tag{8}$$

Hence, if the forces are known, the viscosity at an elevated temperature, $\mu_g(T_{film})$, can be calculated from Eq. (7), yielding the film temperature [1,14], and leading to particle temperature T_p. The accuracy of this procedure has been extensively discussed in the previous studies [12].

Using this approach, the particle temperature levels were estimated. The maximum particle temperatures in the present experiments were 530 and 600 K for the assisting and opposing regimes, respectively.

Uniformity of particle temperature has been checked using the Biot number, *Bi*. From the manufacturer's data, thermal conductivity of glassy carbon was correlated as $k_p(T) = 0.817T^{0.376}$ in the range 300–1200 K. It has been shown in Part I [1] that the Nusselt number was typically about 2.3, being close to its pure conduction value. Accordingly, the Biot number for a glassy carbon particle was about 10^{-2}, indicating that particle temperature in all the experiments was uniform.

As shown above, the temperature levels were estimated for the case where the free convection was fully suppressed by the forced flow. It has been shown in Part I of the present study [1] that the estimated values reflect quite accurately also the temperatures for the free-convection-dominated and intermediate regimes.

It has been also shown in [1] that the film-temperature Grashof number, $Gr_f = g\beta_f(T_p - T_{cold})d^3/v_f^2$, where v is the kinematic viscosity of the gas, and β is the coefficient of thermal expansion, is almost the same over the given range of the particle temperatures. Thus, a small deviation of the particle temperature from the estimated value does not have any effect on it. Because of such behavior of the Grashof number, the characteristic film-temperature Reynolds number, defined from $Re_f/Gr_f^{1/2} = 1$, is almost constant.

Since the film-temperature Grashof number, Gr_f, is essentially the same in the experiments, it should not be used for generalization of the results. Instead, as shown previously [1], the relative temperature difference $(T_p - T_{cold})/T_{cold}$ is suitable for the analysis of the results. There, it was assumed that at the entire range of $0 < Re_p < 0.5$, the drag force along the flow direction is a superposition of two factors, namely, the Stokes-like drag based on the film temperature, and the additional force arising from free convection:

$$F_d = 3\pi d\mu_g(T_{film})u + F_{d,free}. \tag{9}$$

Dividing Eq. (9) by $F_{d,cold} = 3\pi d\mu_g(T_\infty)u$ and rearranging terms, one obtains the contribution of free convection to the forced-flow drag as

$$\frac{F_{d,free}}{F_{d,cold}} = \frac{F_d}{F_{d,cold}} - \frac{\mu_g(T_{film})}{\mu_g(T_\infty)}. \tag{10}$$

Based on this result, a 5/4-power law has been applied in Part I to the analysis of the drag force as a function of the particle temperature. It has been shown there that, for the cross-flow configuration, representation of the experimental data in the form of $[F_d/F_{d,cold} - \mu_f/\mu_{cold}]/[(T_p - T_{cold})/T_{cold}]^{5/4}$ versus Re_{cold} brought the points measured for different heating levels to a single curve.

Since the phenomena of assisting and opposing flows have essentially the same physical nature as that of the cross-flow, exactly the same approach is adopted here for the assisting and opposing configurations. Fig. 8 represents the generalized results for the assisting flow in the form of $[F_d/F_{d,cold} - \mu_f/\mu_{cold}]/[(T_p - T_{cold})/T_{cold}]^{5/4}$ versus Re_{cold}. One can see that all the measured points tend to form a single curve, notwithstanding the heating level. The generalized result indicates clearly that the force acting on a heated particle decreases monotonically to its asymptotic value determined by the modified Stokes law, Eq. (6).

Fig. 9 represents the generalized results for the opposing flow in the form of $[F_d/F_{d,cold} - \mu_f/\mu_{cold}]/[(T_p - T_{cold})/T_{cold}]^{5/4}$ versus Re_{cold}. Once again, all the measured points tend to form a single curve, notwithstanding the heating level.

The results of Figs. 8 and 9, along with those presented in Part I, indicate that a general dependence of the drag force, acting on a heated sphere, on the hydrodynamic and thermal parameters of the system is feasible. The only parameter not used yet is the angle φ between the directions of the free and forced flows. This

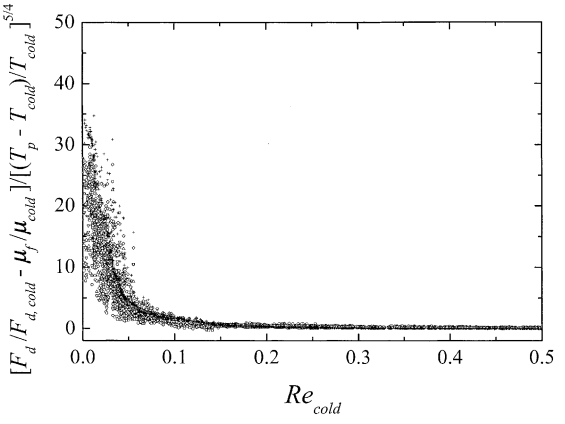

Fig. 8. Assisting flow: the temperature-normalized drag force ratio, as a function of the "cold" particle Reynolds number.

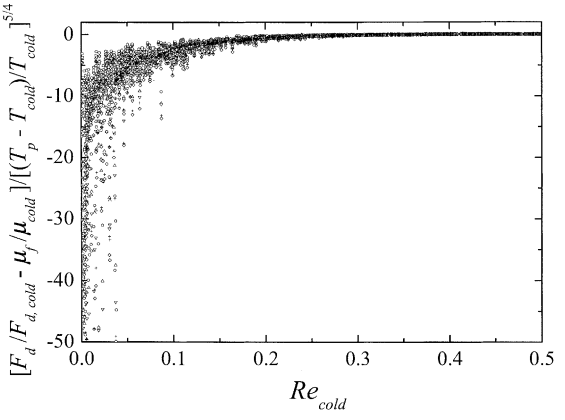

Fig. 9. Opposing flow: the temperature-normalized drag force ratio, as a function of the "cold" particle Reynolds number.

angle determines the differences in the shape of the generalized curve for different flow configurations.

Inspection of the expression for the dimensionless temperature used above, $(T_p - T_{cold})/T_{cold}$, shows that it can be considered as a component of the Grashof number, when the latter is based on the ambient temperature, $T_\infty = T_{cold}$, rather than on the film temperature T_{film}. Recall that for an ideal gas, the coefficient of volumetric expansion, β, is the inverse of the absolute gas temperature. Thus, if the Grashof number is defined based on the ambient temperature, it attains the following form:

$$Gr_\infty = \frac{g\beta_\infty (T_p - T_{cold}) d^3}{\nu_\infty^2} = \frac{(T_p - T_{cold})}{T_{cold}} \frac{g d^3}{\nu_\infty^2}. \tag{11}$$

Since the term gd^3/ν_∞^2 is a constant, the expression $(T_p - T_{cold})/T_{cold}$ is, essentially, analogous to the ambient-temperature Grashof number, and the latter can replace the former in the data generalization. As a result, the generalized force would be expressed as $[F_d/F_{d,cold} - \mu_f/\mu_{cold}]/Gr_\infty^{5/4}$ versus Re_∞. The latter form is probably preferable as it includes the basic dimensionless groups explicitly. Note that although both the Reynolds and Grashof numbers are based on the ambient temperature, the influence of particle heating expresses itself in the viscosity.

As mentioned above, the classical work by Hieber and Gebhart [10] presents a unique attempt to solve the problem of creeping-flow mixed convection analytically. They considered the assisting and opposing configurations for $Gr = o(Re^2)$ as $Re \to 0$, and found the additional drag, related to the free convection, in terms of the small parameter $\varepsilon = Gr/Re^2 = o(1)$, and the Reynolds number Re.

Since the ratio of the overall drag acting on a heated particle to that acting on the cold one under the otherwise same conditions equals, in our notation, to $F_d/F_{d,cold}$, the latter expression is plotted in Fig. 10 versus the particle Reynolds number. It is important to note that we assume that the drag coefficient found by Hieber and Gebhart [10] tends asymptotically to its value for a hot particle with suppressed free convection, i.e. to the value corresponding to the drag force determined by Eq. (8).

Our experimental data for the assisting flow are represented for the different heating levels. The analytical prediction of Hieber and Gebhart [10] is shown for the estimated minimum and maximum Grashof numbers of the present experiments, i.e. $Gr_\infty = 0.006$ and $Gr_\infty = 0.016$, respectively. These values of the Grashof number correspond to the lower and upper sets of the experimental results for the assisting flow. Note that both the Grashof and Reynolds numbers were defined by Hieber and Gebhart [10] using particle radius rather than its diameter. Here, their expression has been transformed to be consistent with the definitions of the present study.

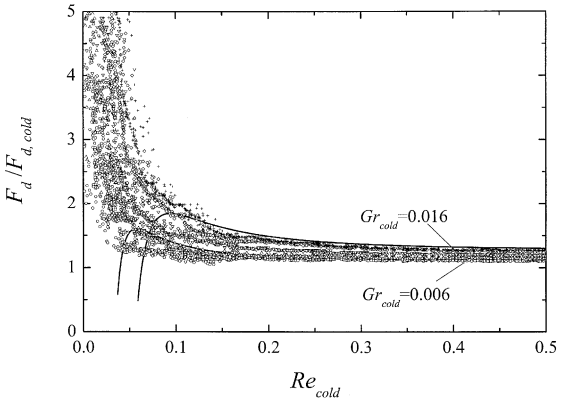

Fig. 10. Comparison of the experimental results to theoretical predictions by Hieber and Gebhart [10]. The theoretical predictions are shown by solid lines for different Grashof numbers.

One can see that at the relatively large Reynolds numbers, the asymptotic solution agrees quite well with the experimental data. However, at the small values of Re the asymptotic solution deviates considerably from the experimental results.

Recall that the solution of Hieber and Gebhart [10] is valid when $Gr/Re^2 = o(1)$. However, it should be noted that for $Gr_\infty = 0.006$ and $Gr_\infty = 0.016$, the characteristic ambient-temperature Reynolds number, defined from $Re_\infty/Gr_\infty^{1/2} = 1$, is as large as about 0.055 and 0.09, respectively, when calculated using their radius-based definitions for Re and Gr. Furthermore, if the condition is rewritten as $Gr/Re^2 < 0.1$, the Reynolds number should exceed 0.18 and 0.29, respectively, to define the regions in which the asymptotic solution is valid. For this reason, the higher the Grashof number, the wider (starting from zero) the range of the Reynolds numbers in which the asymptotic solution cannot be used for an accurate prediction of the experimental results.

4. Closure

The present investigation provides novel qualitative and quantitative results concerning the complex issue of mixed convection in the assisting and opposing flow around a sphere. It is shown how the free and forced convection interact both when one of them dominates over the other, and when there are comparative contributions of both.

Comparison with analytical predictions from the literature has been performed, and the limitations of the existing asymptotic model were discussed.

A power law, established in the previous investigation for the cross-flow, has been successfully applied to the assisting and opposing configurations. Thus, the generalization of all three basic flow configurations in

mixed convection is achieved. This generalization relates the hydrodynamic drag force, acting on a heated sphere, to the Grashof and Reynolds numbers.

References

[1] G. Ziskind, B. Zhao, D. Katoshevski, E. Bar-Ziv, Experimental study of the forces associated with mixed convection from a heated sphere at small Reynolds and Grashof numbers – Part I: Cross flow, Int. J. Heat Mass Transfer 44 (2001) 4381–4389.

[2] J.J. Mahony, Heat transfer at small Grashof number, Proc. R. Soc. London A 238 (1956) 412–423.

[3] F.E. Fendell, Laminar natural convection about an isothermally heated sphere at small Grashof number, J. Fluid Mech. 34 (1968) 163–176.

[4] M.A. Hossain, B. Gebhart, Natural convection about a sphere at low Grashof number, in: Fourth International Heat Transfer Conference, Versailles, vol. 5, 1970.

[5] F. Geoola, A.R.H. Cornish, Numerical solution of steady-state free convective heat transfer from a solid sphere, Int. J. Heat Mass Transfer 24 (1981) 1369–1379.

[6] F. Geoola, A.R.H. Cornish, Numerical simulation of free convective heat transfer from a sphere, Int. J. Heat Mass Transfer 25 (1982) 1677–1687.

[7] B. Gebhart, Y. Jaluria, R.L. Mahajan, B. Sammakia, Buoyancy-Induced Flows and Transport, Hemisphere, New York, 1988.

[8] D.R. Dudek, T.H. Fletcher, J.P. Longwell, A.F. Sarofim, Natural convection induced drag forces on spheres at low Grashof numbers: comparison of theory with experiment, Int. J. Heat Mass Transfer 31 (1988) 863–873.

[9] T. Yuge, Experiments on heat transfer from spheres including combined natural and forced convection, ASME J. Heat Transfer 82 (1960) 214–220.

[10] C.A. Hieber, B. Gebhart, Mixed convection from a sphere at small Reynolds and Grashof numbers, J. Fluid Mech. 38 (1969) 137–159.

[11] T.S. Chen, B.F. Armaly, Mixed convection in external flow, in: S. Kakac, R.K. Shah, W. Aung (Eds.), Handbook of Single-Phase Convective Heat Transfer, Wiley, New York, 1987.

[12] B. Zhao, D. Katoshevski, E. Bar-Ziv, Temperature determination of single micrometre-sized particles from forced/free convection and photophoresis, Meas. Sci. Technol. 10 (1999) 1222–1232.

[13] D. Katoshevski, B. Zhao, G. Ziskind, E. Bar-Ziv, Experimental study of the drag force acting on a heated particle, J. Aerosol Sci. 32 (2001) 73–86.

[14] Y.S. Touloukian, C.Y. Ho, Thermophysical Properties of Matter, The TPRC Data Series, vol. 3, Thermophysical Properties Research Center, Purdue University, 1970.